Remote Sensing of Environment 140 (2014) 46–59

Contents lists available at ScienceDirect

Remote Sensing of Environment

journal homepage: www.elsevier.com/locate/rse

Comparison of different BRDF correction methods to generate daily normalized MODIS 250 m time series

Diego de Abelleyra [a,*], Santiago R. Verón [a,b]

[a] Instituto de Clima y Agua, Instituto Nacional de Tecnología Agropecuaria (INTA), N. Repetto y de los Reseros SN, 1686 Hurlingham, Argentina
[b] CONICET, Argentina

ARTICLE INFO

Article history:
Received 31 July 2012
Received in revised form 13 August 2013
Accepted 14 August 2013
Available online 19 September 2013

Keywords:
Surface reflectance
Directional effects
Hyper-temporal
Crop monitoring MODIS 250 BRDF

ABSTRACT

Realizing the full benefits of MODIS' temporal resolution requires, among others, the correction of the directional effect (i.e. the combined impact of the variation of the measurement geometry and of the observed land surface upon the registered radiant flux). While different BRDF methods have been proposed to address this effect, its performance has been evaluated at coarse spatial resolutions making it difficult to assess its applicability to, for example, crop monitoring. Here we test 2 approaches based on two different assumptions: the Classic approach that relies on the hypothesis of stable target and a recent Alternative that is based on the idea that despite reflectance magnitude may change rapidly, the BRDF shape varies slowly in time. Additionally, we segmented the growing season into different numbers of periods for the BRDF correction (a single period along the growing season, 3 periods based in phenology and 9–12 periods of fixed 16-days). The resulting 6 methods were compared over annual crops (wheat, maize and soybean) at 250 m spatial resolution from a site located in the Argentine Pampas. We used MOD and MYD 09 GQ and GA as inputs and compared the corrected daily red and infrared reflectances and the NDVI time series against the filtered benchmark (input time series with quality filters applied) by means of the high frequency variability (i.e. noise). We also tested whether corrected time series were better correlated with soybean PAR interception and biomass. Our results showed that methods' performance was more explained by the number of periods than by the approach (Classic or Alternative). Single period methods decreased noise by 52%, 55% and 4% for red, infrared and NDVI time series. The use of 3 periods improved the correction performance to 63, 64 and 24% for red, infrared and NVDI time series respectively, while the highest reductions (65, 68 and 32% for red, infrared and NVDI) were found with 16-day intervals (9–12 periods) considering a magnitude inversion process. Wheat displayed the lowest noise reduction compared to the other crops. BRDF parameters obtained from different methods were associated to crop structure, suggesting that they have biophysical meaning. The decrease in noise obtained with correction methods was translated into a better assessment of the fraction of intercepted PAR and biomass. These promising results suggest the possibility of extensive field crop monitoring at an unprecedented temporal resolution.

1. Introduction

Earth observing satellites have played a central role in the generation of global datasets that led to an unprecedented understanding of the functioning of the Earth system. In particular, the MODerate-resolution Imaging Spectroradiometer (MODIS) mission datasets span more than 10 years of near-daily observations of the entire Earth surface radiant flux acquired in 36 spectral bands ranging the visible to infrared spectra at 1 km, 500 and 250 m nadir pixel resolutions (Salomonson et al., 2011). After applying different processing algorithms this huge amount of data gives way to more than 40 geophysical products which have served to observe and monitor key land, atmosphere, and ocean variables and to foster hypothesis testing. Examples range from radiation budgets (e.g. Kaufman, Tanré, & Boucher, 2002), ecosystem process — including vegetation phenology (e.g. Zhang et al., 2003) and fire occurrence (e.g. Van Der Werf et al., 2006), land cover characterization (e.g. Friedl et al., 2002) and agriculture (Becker-Reshef, Vermote, Lindeman, & Justice, 2010; Pittman, Hansen, Becker-Reshef, Potapov, & Justice, 2010) to aerosol, cloud and precipitable water assessment (e.g. King et al., 2003) and ocean chlorophyll content (e.g. Darecki & Stramski, 2004) among others.

There are, however, certain aspects of the MODIS datasets that have not been completely exploited. The temporal resolution may be one of these aspects as most MODIS products are generated at 8 and, mostly, 16 day intervals. This decrease in the temporal resolution of global products is mainly due to the presence of clouds and aerosols in addition to the directional effect. The directional effect refers to the

* Corresponding author. Tel./fax: +54 1146211684.
E-mail addresses: ddeabelleyra@cnia.inta.gov.ar (D. de Abelleyra), sveron@cnia.inta.gov.ar (S.R. Verón).

0034-4257/$ – see front matter © 2013 Elsevier Inc. All rights reserved.
http://dx.doi.org/10.1016/j.rse.2013.08.019

combined impacts of the variation of the illuminating and viewing geometries and of the observed land surface upon the registered radiant flux (Rasmussen, Göttsche, Olesen, & Sandholt, 2011). This means that differences between satellite observations in two clear consecutive days could be a consequence of potential changes in the physical properties of the surface and of variations in the viewing and illuminating geometries. Hopefully, new methodologies (Breon & Vermote, 2012; Vermote, Justice, & Breon, 2009) may ease the limitations imposed by directional effects with processing requirements compatible with large daily 250 m datasets. Here we compare different methodologies to correct directional effects in MODIS daily data from an agricultural area in the Pampas region of Argentina.

The scattering of a parallel beam of incident light from one direction into another direction after interacting with a surface is described by a Bidirectional Reflectance Distribution Function (BRDF) (Schaepman-Strub, Schaepman, Painter, Dangel, & Martonchik, 2006). By considering variables that characterize the viewing and illumination geometries (i.e. sun zenith angle, view zenith angle, and both azimuths with respect to a reference direction) the BRDF allows isolation of the surface intrinsic reflectance properties from those related to the observation geometry. Therefore, a model able to reproduce a target BRDF is needed to correct for directional effects. Though many different models have been proposed, we will focus on the one use by the MODIS mission (Schaaf et al., 2002) and a recent method proposed by Vermote et al. (2009).

The BRDF correction methodology currently implemented in the MODIS BRDF/Albedo product (MCD43) is based on a linear model with two functions (i.e. kernels) and three parameters (i.e. kernel weights). This type of model was originally proposed by Roujean, Leroy, and Deschamps (1992) and subsequently modified to account for different processes such as the hot-spot (Breon, Maignan, Leroy, & Grant, 2002; Li & Strahler, 1992). The kernels' formulation in use in the MCD43 product were developed by Ross (1981) (i.e. Ross—thick) and by Li and Strahler (1992) (Li—sparse) (Schaaf et al., 2002). This model (hereafter "Classic approach"), estimates reflectance (ρ) as the sum three terms:

$$\rho(\theta_s,\theta_v,\phi) = k_0 + k_1 F_1(\theta_s,\theta_v,\phi) + k_2 F_2(\theta_s,\theta_v,\phi) \quad (1)$$

where F_1 and F_2 (i.e. kernels) are the analytical functions of the solar or illumination (θ_s), relative azimuthal (Φ) and viewing angles (θ_v) and k_x are kernel weights. The first term (isotropic term) is comprised of k_0 which represents the bidirectional reflectance for $\theta_s = \theta_v = 0$. The second ($k_1{}^* F_1$) and the third terms ($k_2{}^* F_2$) represent the geometric and volumetric scattering contributions to the surface reflectance respectively. According to Roujean et al. (1992) parameters k_0, k_1 and k_2 depend, among other factors, on the shape and distribution of the objects in the surface and the expected proportion of geometric and volumetric contributions. In particular, k_1 is related to the height, length, horizontal area and Lambertian reflectance of surface protrusions while k_2, in the case of vegetated surfaces, is mainly related to leaf area index (LAI) of the canopy. Although kernel parameters should be related to target characteristics (e.g. LAI or geometric features) the extent to which they can provide valuable information about surface properties has been scarcely evaluated (Gao, Schaaf, Strahler, Jin, & Li, 2003; Roujean et al., 1992; Vermote et al., 2009).

For the MCD43 product, k_0, k_1 and k_2 are estimated by minimization of the sum of the square difference between estimated and observed reflectance over a 16-day revisit period (Schaaf et al., 2002). In the cases where less than 7 good quality observations are registered, a magnitude inversion is performed — BRDF parameters are obtained from a look up table. The 16 day period represents a trade-off between obtaining sufficient good quality observations (i.e. free of clouds, aerosols and viewing angles lower than 60°) and violating the assumption that the target remains stable (unchanged) during the period. For annual crops in particular the assumption of stable target might be unrealistic and may lead to errors (Vermote et al., 2009).

Vermote et al. (2009) proposed an alternative approach (hereafter "Alternative approach") to correct for directional effects which accounts for surface changes through time. Their method is based on the assumption that despite reflectance magnitude may change rapidly, the BRDF shape varies slowly in time implying that k_1 and k_2 stay proportional to k_0. Translated into a mathematical form, they factorized Roujean et al. (1992) model so that:

$$\rho(\theta_s,\theta_v,\phi,t) = k_0(t)[1 + VF_1(\theta_s,\theta_v,\phi) + RF_2(\theta_s,\theta_v,\phi)] \quad (2)$$

being R the roughness (k_1/k_0) and V the volumetric (k_2/k_0) parameters respectively. In turn, the assumption of negligible change in BRDF shape between successive observations – $p(t_i)$ and $p(t_{i+1})$ – allowed Vermote et al. (2009) to estimate R and V by minimizing the sum of the square difference between the following 2 terms:

$$k_{0i} \approx k_{0i+1} \quad \text{or} \quad \frac{\rho(t_i)}{[1 + VF_1^i + RF_2^i]} \approx \frac{\rho(t_{i+1})}{[1 + VF_1^{i+1} + RF_2^{i+1}]} \quad (3)$$

where i stands for time. As with the Classic, the outcome of the Alternative approach is a new set of normalized reflectance time series to standard observation geometry.

Using this method Vermote et al. (2009) reported a significant decrease in the high frequency variability – i.e. "noise" – of MODIS daily time-series from 25 km^{-2} pixels corresponding to different land covers/uses — savanna, evergreen forest, deciduous forest and broadleaved crops. With a refinement of this methodology – i.e. allowing the correction to operate at sub-periods of varying length – at the savanna site the noise reduction amounted to 82, 86 and 58% for the red and infrared bands and the NDVI respectively. Additionally, these authors concluded that the global patterns of parameters R and V were consistent with land cover suggesting that these parameters might carry valuable geophysical information. On a different setting, Becker-Reshef et al. (2010) capitalized this dataset to develop a generalized approach to estimate wheat yields at 0.05° spatial resolution with an error lower than 10%. Despite these promising results this methodology remains to be tested at a finer spatial resolution to assess its potential to improve the monitoring of vegetation dynamics.

The objective of this study is to test different methods to correct directional effects in MODIS reflectance time series over annual crops (wheat, maize and soybean) at 250 m spatial resolution. We specifically seek to answer the following questions: which method performs better? How important is the length of the periods used to characterize the BRDF? Is there an interaction between method and crop? Are the model parameters associated to any crop feature? Does corrected time series improve our ability to derive valuable crop information such as biomass or fraction of intercepted radiation? Answering these questions is a key step towards realizing the potential of daily MODIS data to monitor crops at 250 m spatial resolution. Vegetation indexes provided by the MOD 13 and MYD 13 products have a time step of 16 days and are generated using reflectance registered in one given day within that 16 day interval (Huete, Didan, van Leeuwen, Miura, & Glenn, 2011).

2. Materials and methods

Satellite and field information corresponded to an agricultural area located in San Antonio de Areco department (34° 14′S 59° 33′W) in Buenos Aires province, Argentina. MODIS Terra and Aqua daily reflectance products (MOD09GQ/GA and MYD09GQ/GA, tile h13 v12) were downloaded from NASA REVERB website (http://reverb.echo.nasa.gov/reverb/). Field level crop data from 2007 to 2011 (crop type — maize, wheat, early soybean, late soybean) were obtained from local farmers. During 2011–2012 we conducted several field campaigns to monitor crop biomass focusing on early and late soybeans.

We applied different BRDF correction methods to the same quality filtered surface red and infrared reflectance MODIS observations. Although differences between methods, each correction coarsely consisted on a) model parameters retrieval and b) normalization of observed reflectance to the same viewing and illumination geometry using the model parameters obtained in a). Then we evaluated each correction method by means of an estimate of the noise (i.e. high frequency variability, Vermote et al., 2009), a comparison between modeled and LANDSAT reflectance, RMSE of model fit and the angular sampling distribution. Also, we evaluated the ability of each normalized dataset to estimate the fraction of intercepted PAR (fIPAR) and biomass from early and late soybeans. Finally, we performed an analysis of sensitivity to assess the effect of different quality filters upon method performance.

BRDF corrections were carried out only on pixels whose area was occupied by at least 95% by a single crop. For each crop (i.e. wheat, maize, early soybean and late soybean) we defined a growing season based on local average sowing and harvesting dates. Thus, we corrected the red and infrared reflectances and calculated the NDVI on a crop growing season basis for a total of 2628 pixels belonging to 4 different crops distributed over 48 fields in 4 agricultural campaigns and considering two sensors (Aqua and Terra).

2.1. BRDF correction methods

The BRDF correction approaches we used include 2 methodologies already published (Schaaf et al., 2002 — Classic approach; Vermote et al., 2009 — Alternative approach) applied over different lengths (number) of periods. Thus, we segmented the growing season into periods wherein changes in vegetation characteristics are expected to be minimum. Therefore, BRDF parameters were retrieved at a single-period (i.e. crop growing season) or multiple-periods (i.e. 3 periods within the growing season based on phenology or 9–12 periods of fixed 16 days to match that of the MCD43 product). The resulting methods were: 1) Classic single-period (Classic SP), 2) Classic 3 multiple-periods (Classic 3MP), 3) Classic 9–12 multiple-periods (Classic 12MP), 4) Alternative single-period (Alternative SP), 5) Alternative 3 multiple-periods (Alternative 3MP) and 6) Alternative 9–12 multiple-periods (Alternative 12MP). A magnitude inversion was performed whenever a period from the 12MP method had less than 7 good quality observations. This inversion involved the use of the corresponding BRDF parameters from the 3MP method.

2.2. Normalization

Once the 6 sets of BDRF parameters – corresponding to the 6 correction methods – were obtained, we normalized observed red and infrared reflectances (ρ^N) to a common observation geometry (i.e. 45° illuminating angle, 0° viewing angle — nadir, and 0° relative azimuthal angle). This normalization was performed by multiplying the observed reflectance (ρ') by the ratio between modeled normalized reflectance – obtained with each method (using the estimated parameters) – and modeled observed reflectance (using observed viewing, illuminating and azimuthal angles).

$$\rho^N = \rho' \frac{k_0 + k_1 F_1^N + k_2 F_2^N}{k_0 + k_1 F_1 + k_2 F_2} \tag{4}$$

and

$$\rho^N = \rho' \frac{1 + RF_1^N + VF_2^N}{1 + RF_1 + VF_2} \tag{5}$$

for the Classic and Alternative methodologies respectively.

2.3. Correction method evaluation

We assessed the performance of each correction method by means of the high frequency variability (i.e. noise) (Breon & Vermote, 2012; Vermote et al., 2009). Additionally, we estimated the root mean square error (i.e. RMSE) of the model fit and compared the corrected time series with observed reflectance from LANDSAT images. To account for possible differences in input data quality, we calculated the Weight of Determination (Lucht & Lewis, 2000).

2.3.1. High frequency variability

Following Vermote et al. (2009) we evaluated the impact of each correction method by computing an estimate of the high frequency variability (i.e. noise). Noise value is derived from the difference between the center observation from a triplet (tree successive observations, $i, i+1$ and $i+2$) and the estimated value assuming a linear interpolation between the two extremes:

$$Noise(y) = \sqrt{\frac{\sum_{i=1}^{n-2}\left(y_{i+1} - \frac{y_{i+2}-y_i}{day_{i+2}-day_i}\left(day_{i+1}-day_i\right)-y_i\right)^2}{N-2}} \tag{6}$$

where y_x stands for observed reflectance or NDVI in a given day ($i, i+1$, or $i+2$).

As formulated, this measure of noise would scale with the mean of the observations. Therefore, to compare the noise from crops with different average reflectance or NDVI values, we also calculated a relative noise as:

$$NoiseR(y) = \frac{1}{\sqrt{N-2}}\sqrt{\sum_{i=1}^{n-2}\left(\frac{\left[y_{i+1} - \frac{y_{i+2}-y_i}{day_{i+2}-day_i}\left(day_{i+1}-day_i\right)-y_i\right)\right]}{y_{i+1}}\right)^2}. \tag{7}$$

2.3.2. Model fit

The root mean square error (RMSE) is an extensively used measure of the uncertainty of model predictions. We here used the RMSE as a descriptor of the differences between the observed reflectance from MODIS (i.e. the filtered time-series) and the BRDF corrected reflectance modeled at the same measurement geometry of the observed reflectance. Thus, as RMSE increases so does the uncertainty in the model-fits.

2.3.3. Modeled vs. observed reflectance

We compared MODIS Terra and Aqua reflectance values obtained with different correction methods vs. reflectance obtained with a near nadir viewing system as LANDSAT. We used 6 LANDSAT TM cloud free acquisitions (scene 226-84) including different agricultural campaigns and times during a year (Table 1). Digital numbers were converted to radiance and reflectance following Chandler and Markham (2003) and Rayleigh atmospheric corrections were applied according to Stumpf (1992). MODIS data were modeled to illumination and viewing geometries of each LANDSAT scene. LANDSAT viewing angle was assumed as

Table 1
Illumination (θ_s), viewing (θ_v) and relative azimuthal (Φ) angles for LANDSAT (path: 226, row: 84), Terra and Aqua on the dates considered for the validation.

Date	LANDSAT	Terra			Aqua		
	θ_s	θ_s	θ_v	Φ	θ_s	θ_v	Φ
10/22/2008	37.8	39.9	61.6	−43	34.7	37.4	−138.4
01/26/2009	38.4	40.9	61.6	−28	25.2	37.1	−139.8
03/15/2009	48.3	50.5	61.6	−47.1	39	37.6	−121.8
09/23/2009	46.3	49	61.6	−52.4	42.3	36.9	−125.2
01/13/2010	35.1	38.9	61.7	−24.9	23.7	36.9	−146.1
03/21/2011	49	51.9	61.5	−49.4	40.5	36.8	−119.3

0° for all the scenes. We computed the RMSE between MODIS modeled reflectance and LANDSAT reflectance averaged across all pixels within the area of each MODIS pixel.

2.3.4. Weight of Determination

The Weight of Determination (WoD) quantifies the sensitivity of the correction model parameters (and of the corrected reflectance) to the angular sampling of the observed data (Lucht & Lewis, 2000). A high WoD is indicative of a poor angular sampling. It has been extensively used in BRDF correction attempts and Albedo retrieval studies (Chopping, 2000; Roy, Lewis, & Justice, 2002; Schaaf et al., 2002; Shuai, Schaaf, Strahler, Liu, & Jiao, 2008) as a quality indicator of input data. As suggested by the literature, we calculated the WoD for a given parameter u as:

$$\mathrm{WoD}_u = [U]^T \left[M^{-1}\right] \cdot [U] \quad (8)$$

where U is a vector composed of the terms u_i (being i the number of the model kernels), and M^{-1} is the inverse matrix providing the analytical solution of inversion equations. For each crop, we computed the WoD for the resulting reflectance for the Classic single and multiple-period correction approaches.

2.4. Correlation with biophysical variables

We assessed if the corrected time series were better related to biophysical parameters from vegetation by regressing a) NDVI vs. fIPAR from specific dates and b) maximum NDVI from each correction method vs. soybean peak dry-biomass. To that end, during the 2011–2012 agricultural campaign we measured fIPAR in soybean fields by means of a ceptometer (Cavadevices, Buenos Aires, Argentina). Measurements of PAR over and below the crop canopy were done at full sunny days between 11:00 and 15:00 local time. We also conducted periodic harvests at 12 soybean fields located within the studied area. In each soybean field we harvested ten 0.5 linear meters from a row and registered the distance between rows. Harvests were distributed within soybean fields so as to sample an average of 3 pixels per field. At the laboratory samples were oven dried (more than 72 h at 70 °C) and weighted until constant weight. We used a simple logarithmic regression model to account for the asymptotic relationship between NDVI and biomass. We report the coefficient of determination of both relationships discriminated among correction methods.

2.5. Processing strategy

We first extracted the input data (red and infrared reflectances), observation coverage (Obscov) as well as the angles (viewing, illumination, and azimuth) and quality index from the daily MOD and MYD09 GQ and GA – level L2G – tiles respectively for each crop growing season. Then we discarded observations based on the threshold values for cloud state and aerosol quantity or acquisition geometry shown in Table 2. Given that the resulting set of observations still had suspicious values (e.g. negative reflectance) we further removed outliers (observations lying further than 3 SD from the mean). These *filtered* time-series constituted, then, the input data for the 6 correction approaches.

Table 2
Threshold values used to filter the input data (MOD and MYD09 GQ).

Quality index	Threshold value	Binary value
Viewing angle (°)	<70	–
Sun zenith angle (°)	<70	–
Aerosol quantity	Low	01 and 00
Observation coverage (%)	>5	–
Pixel adjacent to cloud	No	0
Internal cloud algorithm	No cloud	0
Cirrus detected	None	00
Cloud shadow	No	0
Cloud state	Clear	00

Table 3
Dates defining the crop growing season and duration of periods for BRDF correction. 3MP: 3 multiple-periods.

Crop	Growing season start	Initial sub-period end (3MP)	Intermediate sub-period end (3MP)	Growing season end
Wheat	Jul 7	Aug 31	Nov 19	Dec 14
Maize	Sep 20	Nov 24	Feb 24	Mar 24
Early soybean	Oct 20	Dec 25	Mar 9	Apr 4
Late soybean	Dec 14	Feb 4	Apr 4	May 3

Corrections were applied on a per pixel basis. For each crop we considered the complete growing season from sowing to harvest divided in different periods. Periods considered were: a) from sowing to harvest (single period — SP), b) an initial period from sowing to active growth, an intermediate period from active growth to the onset of grain filling and a final period of decreasing growth and senescence (3 multiple-periods — 3MP) and c) a fixed 16 day intervals from sowing to harvest (9–12 multiple-periods — 12MP). It should be noted that the number of fixed 16-day period varied according to the length of each crop growing season (from 9 to 12). Parameters characterizing each crop growing season and duration of periods for BRDF correction are shown in Table 3. Once the parameters were obtained (k_0, k_1 and k_2 for the Classic and V and R for the Alternative methods), we run each model to generate two reflectance sets: one at the normal geometry (45, 0, 0) and another at the observed geometry. The daily ratio of these quantities was used as the correction factor for the daily observed reflectance to obtain the corrected time-series (Eqs. (4) and (5)). Finally, as suggested by Vermote et al. (2009) we performed an outlier removal on these time-series to avoid noise calculation being driven by extreme observations. NDVI was calculated from each corrected red and infrared time-series and also subjected to the outlier removal. To mirror outlier treatments we also performed a second removal on the filtered time series and used this dataset as the benchmark for comparison between correction methods. All the processing was implemented on IDL code (ITT Visual Information Solutions, Colorado, USA).

2.6. Sensitivity analysis

To assess the effect of differences in input data quality over the performance of correction methods, we conducted a sensitivity analysis. For the original 2628 pixels (i.e. 4 crops, 4 years, 2 sensors), 30 additional time series of red and infrared reflectances were generated by considering different threshold values for a given parameter and keeping the others unchanged. Parameter values are shown in Table 4. Each additional time series was fed to the correction approaches and NDVI was then calculated. Finally, noise from red and infrared reflectances and NDVI was computed.

3. Results

In general, BRDF corrections applied to the filtered data yielded reductions in the noise of the time series. As expected, the magnitude of these reductions was different depending on correction method, crop

Table 4
Threshold values considered for the sensitivity analysis.

Parameter	Values
Observation coverage (%)	5–10–15–20–25
Viewing angle (°)	50–55–60–65–70
Sun zenith angle (°)	50–55–60–65–70
Aerosol quantity	Climatology (00)–low (01)–average (10)–high (11)

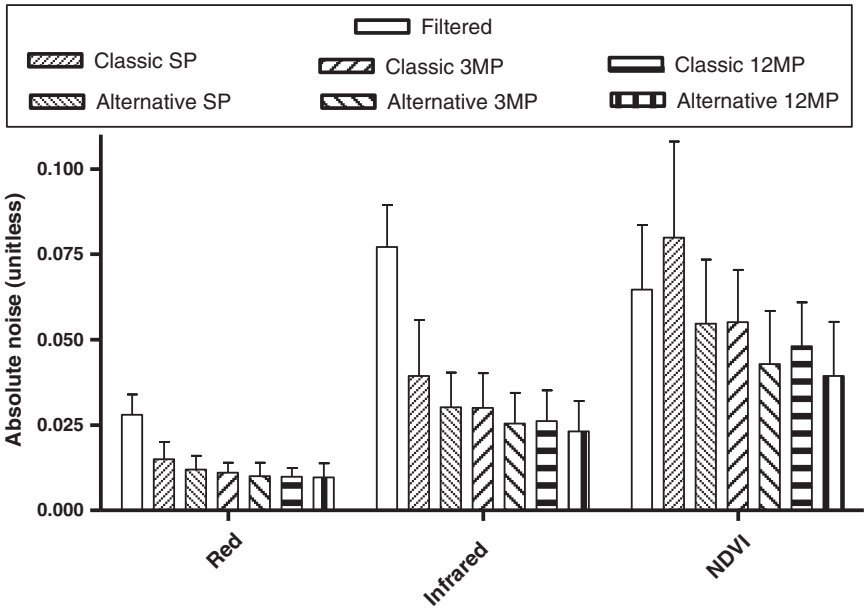

Fig. 1. Median absolute high frequency variability (noise) of filtered (uncorrected) and each correction method for red, infrared and NDVI time-series. SP: single-period, 3MP: 3 multiple-periods, 12MP: 9–12 multiple-periods. Bars represent the median absolute deviation (MAD).

type, and their interaction. The magnitude of the reductions was also different for the red, infrared and NDVI time-series. Model parameters (k_x and R & V) were quite similar among crops and, for each crop, varied consistently in time. Given that the noise distribution was not normal (test Shapiro–Wilk $p \ll 0.05$ for all time series except for filtered infrared band), in the following sections we present the results as median and median absolute deviation discriminated according to method. More parameters (e.g. mean, standard deviation, 5 and 95% percentile, etc.) describing the performance of correction method are given in Appendix 1. Results on a per crop basis are shown in terms of relative noise.

3.1. Comparison between correction methods

Averaged across all crops and years, Classic and Alternative SP correction methods reduced the noise median of the red band by 47 and 56% compared to the filtered time series (0.028 vs. 0.015 and 0.012) (Fig. 1). For the infrared band, reductions were higher. Compared to the filtered time series the reductions amounted to 49 and 61% for the Classic SP and Alternative SP respectively. The Classic SP displayed an increase of 23% in the noise median while the Alternative SP method produced a 15% reduction over the filtered NDVI time series.

When correction methods considered 3 periods (3MP) these reductions further intensified. For the red band each method yielded 61 (Classic) and 63% (Alternative) less noise than the filtered dataset (Fig. 1). For the infrared band the reduction amounted to 61 and 67% for Classic 3MP and Alternative 3MP respectively. NDVI, however, showed a different performance between methods: Classic 3MP achieved a reduction of 15% while for the Alternative it amounted to 34%.

The highest improvement over the filtered time series was observed when 9–12 periods – each of 16 days – (12MP) were used. Time series corrected by the Classic 12MP method showed reductions of 65, 66 and 34% while for the Alternative 12MP achieved reductions of 66, 70 and 39% for the red, infrared and NDVI respectively. Due to the lack of good quality observations, magnitude inversion was applied over 60% of pixels–periods.

The cumulative histogram of the absolute noise for each method (Fig. 2) confirms these results: curves from correction methods lie at the left of the filtered except for the case of the Classic SP for the NDVI. Curves, however, differed on the noise value at which the plateau occurred. In general, for multiple-periods (3MP and 12MP) the plateau of the Alternative methods occurred at higher values of noise and lower cumulative probability than the Classic methods. This indicates that a fraction of the pixels still showed high noise after correction by Alternative compared to Classic methods.

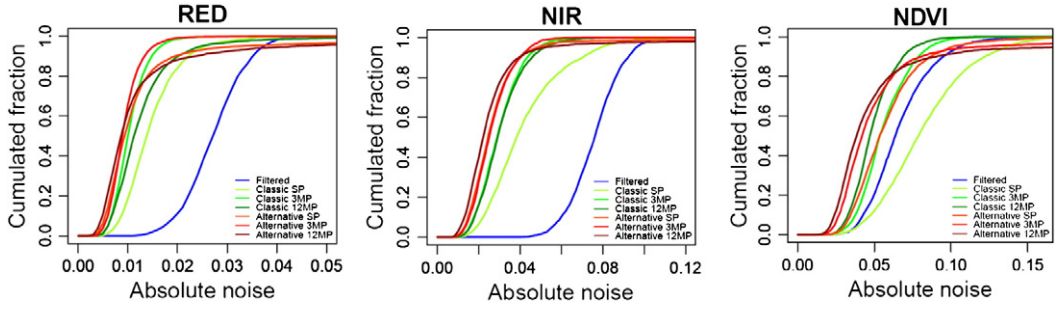

Fig. 2. Cumulative histogram of the absolute noise of the red and infrared reflectances and NDVI time-series for each correction method and filtered (uncorrected) data. SP: single-period, 3MP: 3 multiple-periods, 12MP: 9–12 multiple-periods.

A pixel by pixel analysis showed that correction methods did not performed uniformly. Classic 3MP and 12MP showed improvements (lower noise than uncorrected) in almost 100% of pixels for red and infrared bands. On the contrary, Alternative methods did not imply an improvement in all pixels as, for the red band 91 to 95% of the pixels (12MP and 3MP respectively) displayed lower noise than the filtered time series, while for infrared band this occurred on 97 (12MP) to 99% (3MP). For NDVI the improvement occurred only in 74 to 85% (Classic 3MP and 12MP respectively) and 85 to 88% (Alternative 12MP and 3MP respectively) of the pixels.

Among crops, different performances of correction methods were found at particular combinations of crop and time series. In general wheat showed lower noise reductions than other crops for infrared and NDVI time series (Fig. 3 panels A, B, C). In particular wheat showed lower reductions for Alternative MP methods in red band and for Classic SP in infrared band. Early and late soybean and maize showed, in turn, similar average noise reductions. Coarsely, the pattern of decreasing noise (filtered > SP > 3MP and Classic > Alternative) was maintained among crops. However, for multiple-period correction methods the percentage of improved pixels was slightly lower for wheat (87%) than for

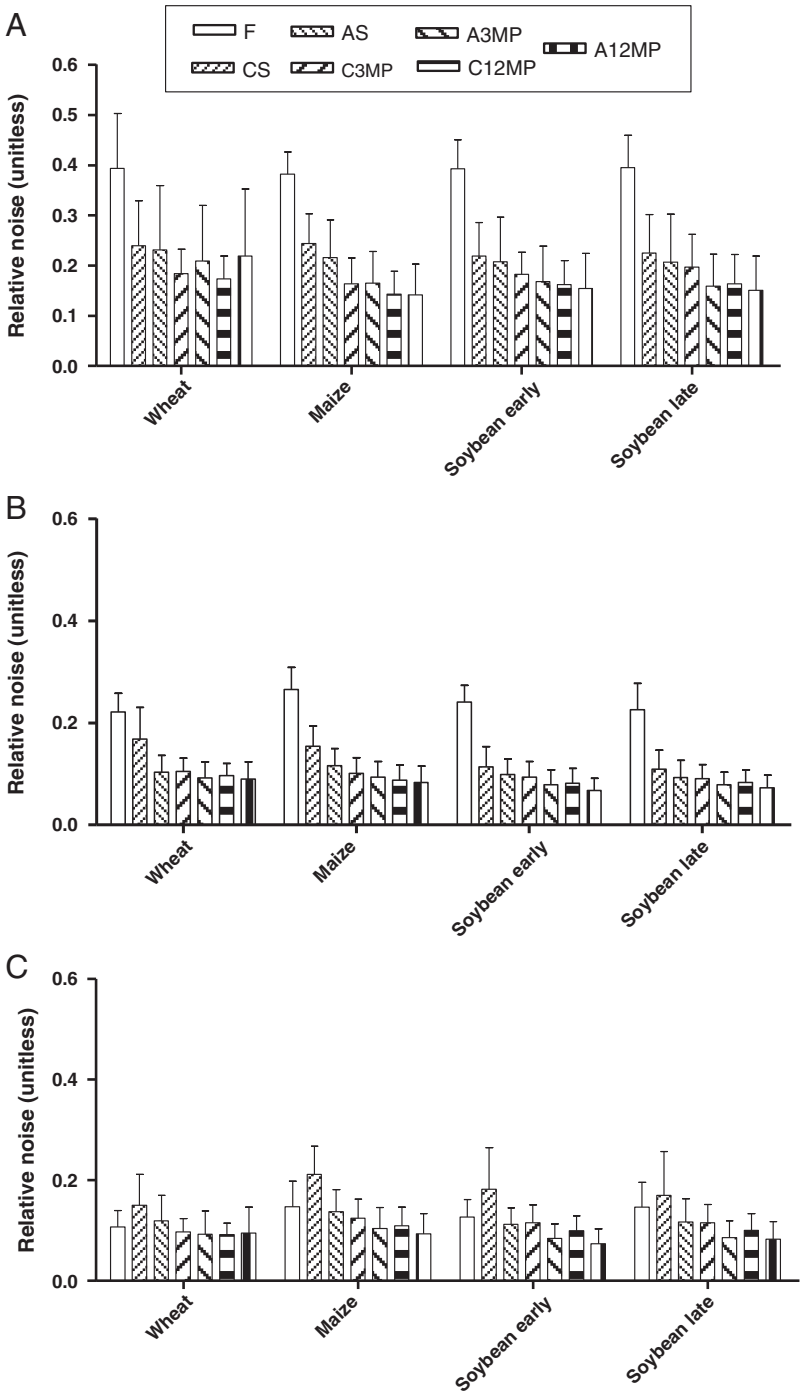

Fig. 3. Median relative high frequency variability (noise) of red (A), infrared (B) and NDVI (C) time series for each crop and correction method. Bars represent median absolute deviation (MAD). SP: single-period, 3MP: 3 multiple-periods, 12MP: 9–12 multiple-periods.

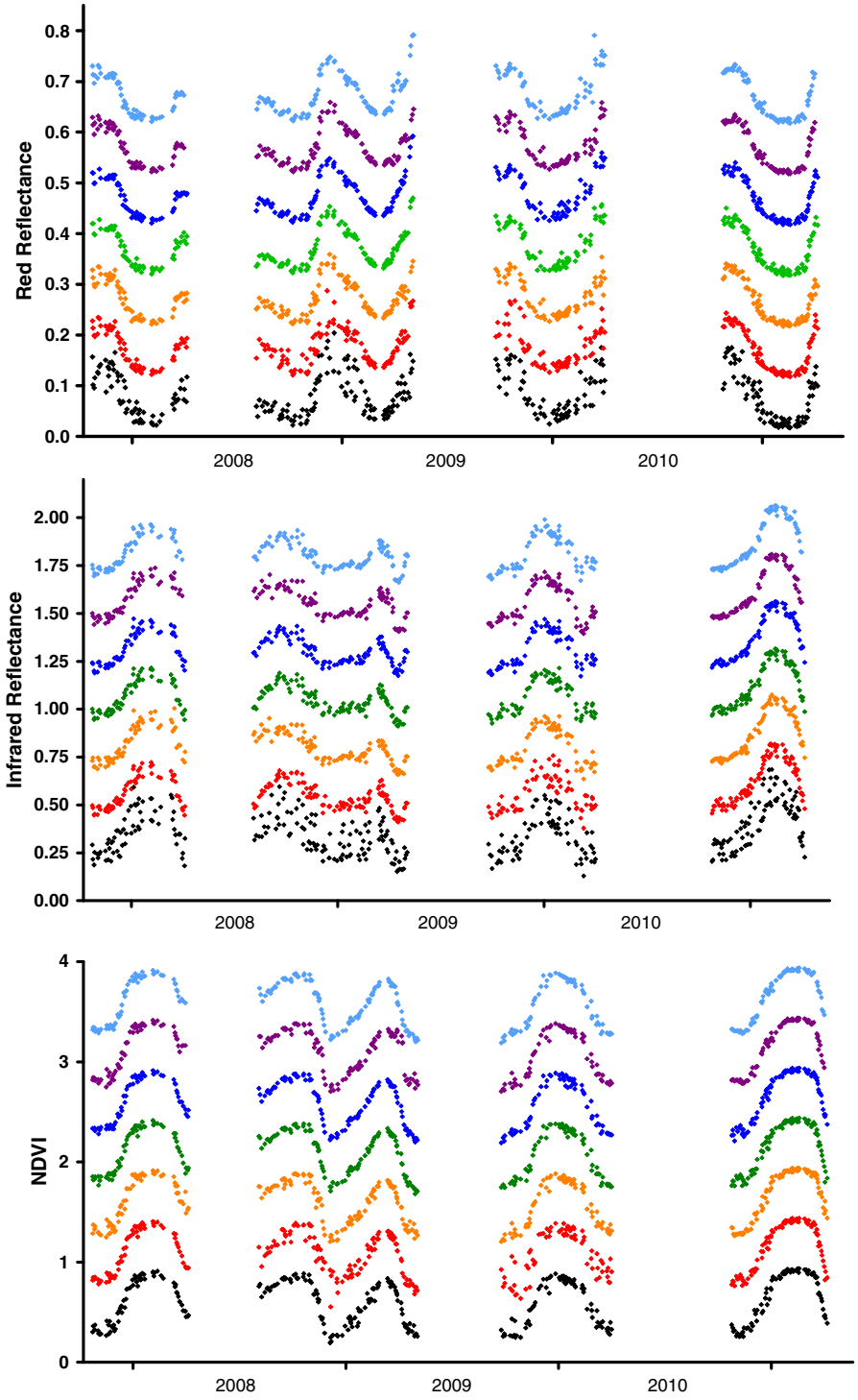

Fig. 4. Time series of MODIS Terra red, infrared and NDVI at a crop field in San Antonio de Areco (Argentina) from 2007 to 2011 in a 4 crop rotation sequence: soybean (2007–2008), wheat–soybean (2008–2009), maize (2009–2010), and soybean (2010–2011). Time series colors: filtered (uncorrected) (black), Classic SP (single period — red), Alternative SP (orange), Classic 3MP (3 multiple-periods — green), Alternative 3MP (blue), Classic 12MP (9–12 multiple-periods — magenta), and Alternative 12MP (cyan). Time series have been shifted by multiples of 0.1, 0.25, and 0.5 for red, infrared, and NDVI, respectively.

Table 5
Median root mean square error (RMSE) of model fit for each correction method. SP: single period, 3MP: 3 multiple-periods, 12MP: 9–12 multiple-periods.

Band	Classic SP	Alternative SP	Classic 3MP	Alternative 3MP	Classic 12MP	Alternative 12MP
Red	0.037	0.016	0.020	0.031	0.016	0.040
Infrared	0.079	0.177	0.044	0.259	0.036	0.239

other crops (94% for early and late soybean respectively, and 97% for maize).

Fig. 4 shows an example of a pixel red, infrared and NDVI MODIS Terra time series filtered and corrected by Classic and Alternative SP, 3MP and 12MP methods. Therein, 4 growing seasons (2007–2011) – corresponding to an agricultural rotation of soybean, wheat/soybean, maize, and soybean – are depicted. The noise reduction associated

Table 6
Root mean square error (RMSE) of LANDSAT red (R) and infrared (IR) reflectance vs. Terra and Aqua data modeled to viewing and illumination geometries of LANDSAT scenes for Classic and Alternative SP, 3MP and 12MP correction methods. RMSE for uncorrected MODIS data (Filtered) was also included. SP: single period, 3MP: 3 multiple-periods, 12MP: 9–12 multiple-periods.

Sensor	Band	Filtered	Classic SP	Alternative SP	Classic 3MP	Alternative 3MP	Classic 12MP	Alternative 12MP
Terra	Red	0.034	0.014	0.011	0.007	0.011	0.005	0.009
	Infrared	0.446	0.123	0.094	0.082	0.063	0.052	0.052
Aqua	Red	0.003	0.005	0.005	0.005	0.008	0.004	0.007
	Infrared	0.064	0.077	0.051	0.048	0.049	0.047	0.053

with the correction methods is evident from the increased grouping – i.e. decrease dispersion – of successive observations particularly for the red and infrared bands.

The median values of the RMSE computed from the modeled reflectance by each of the BRDF correction methods and the observed reflectance – at similar measurement geometry – fell within the range of 0.016 to 0.259 (Table 5). The highest median RMSE was found for the Alternative 3MP for the infrared reflectance and the lowest for the Alternative SP and Classic 12MP for the red reflectance.

The comparison of modeled MODIS vs. LANDSAT reflectance showed RMSE values between 0.004 and 0.014 for red band and between 0.047 and 0.123 for infrared band (Table 6). Alternative SP showed lower RMSE than Classic SP, while Classic multiple-period methods (3MP and 12 MP) showed in general lower RMSE than Alternative 3MP and 12MP. Aqua showed a tendency towards lower RMSE values than Terra as, on average, their viewing angles on dates of LANDSAT acquisitions were lower (Table 1).

Table 7 reports median values of the Weights of Determination (WoD) found for the reflectance corrected by the Classic approach discriminated between crops and periods (SP, 3MP and 12MP). WoD ranged between 0.019 (maize SP) and 16 (wheat, 12MP period 2) being lowest for the SP method (0.026 across all crops) followed by the 3MP (0.169) and highest for the 12MP (0.956). In particular, wheat displayed a high WoD at the beginning of the growing season (markedly high for the first 3 periods of the 12MP and for the initial period of the 3MP method) while, for late soybean the highest value occurred at the end of the growing season (i.e. final sub-period for 3MP or last 2 periods for the 12MP method). For 2391 of 26,592 (9%) combinations of pixel and 16-day periods (12MP), there were less than 3 good quality observations which precluded the application of the correction methods and the WoD calculation.

3.2. Model parameters

Parameters from SP correction methods for infrared time-series were in general higher than for the red time series, and k_2 (volumetric) parameter was higher than k_1 (geometric) for both time-series. However, a clear pattern could not be observed in part because of the high variability displayed by some parameters. In contrast, parameters obtained from 3MP methods had less variability and some consistent patterns emerged. For all crops a decrease in red and an increase in infrared k_0 were observed at the intermediate period (Fig. 5, panels A, B). In the case of infrared k_2 we observed a constant increment for wheat and maize and a hump-shaped pattern for early soybean and particularly late soybean (Fig. 6A).

Similarly to Classic SP parameters, the lack of a clear pattern in *R* and *V* may be due to the high variability in model parameters. *V* parameter was markedly higher than *R* only for the infrared time-series. When parameters were obtained from 3 periods (3MP methods), wheat and maize infrared *V* parameter showed increases through sub-periods (Fig. 6B). Early and late soybeans showed an opposite pattern of decreasing *V* values at intermediate and final periods. As 12MP methods also included a high proportion of 3MP parameters, we excluded these methods from the analysis.

3.3. Relationship between model output and crop biophysical variables

Correlation between daily NDVI and measured fIPAR increased markedly with respect to uncorrected data in most of the correction methods, particularly for all Alternative and Classic 12MP (Table 8). The coefficient of determination for biomass increased between 13 and 15% with the Classic and Alternative SP correction methods. The r^2 improvement was lower when the Classic 3MP and 12 MP methods were considered but the association disappeared when the Alternative 3MP and 12MP were used. However, if the pixels where the correction methods did not result in a noise reduction were excluded from the regressions, the r^2 would notably increase, being in some cases higher than obtained with filtered data (Alternative 3MP and 12MP – Terra and Classic 3MP – Aqua).

3.4. Analysis of sensibility

In general for all time series (red, infrared and NDVI), changes in illumination angle (between 50 and 70°) and aerosol quantity thresholds did not affect noise for the SP and 3MP methods. 12MP methods were not included in this analysis because of the high percentage of pixels that required magnitude inversion. Noise was very sensitive to viewing angle and Obscov thresholds. Comparing each time series, NDVI noise showed higher sensitivity than red and infrared reflectances (data not shown). Single-period methods showed constant decreases in NDVI noise as viewing angle threshold was reduced, but in 3MP methods very low sensitivities were observed (Fig. 7). The number of observations from the filtered time-series decreased from an average of 56 to 40 when the viewing angle threshold changed from 70° to 50°. NDVI noise showed a minimum at intermediate values of Obscov across all correction methods. 3MP methods displayed a higher increase in NDVI noise at high Obscov values than SP methods. In this case, the total number of observations ranged from 56 to 28 between extreme values of Obscov (5 to 25%).

Table 7
Median Weight of Determination of reflectance by each period and method. SP: single period, 3MP: 3 multiple-periods and 12MP: 9–12 multiple-periods. Subscripts indicate the order of each 16-day period in 12MP methods.

Crop	SP	3MP initial	3MP intermediate	3MP final	$12MP_1$	$12MP_2$	$12MP_3$	$12MP_4$	$12MP_5$	$12MP_6$	$12MP_7$	$12MP_8$	$12MP_9$	$12MP_{10}$	$12MP_{11}$	$12MP_{12}$
Wheat	0.033	0.472	0.057	0.143	2.562	16.402	4.638	1.179	0.392	0.366	0.293	0.347	0.246	0.200	–	–
Maize	0.019	0.064	0.038	0.132	0.270	0.318	0.467	0.236	0.193	0.377	0.261	0.213	0.297	0.327	0.445	0.345
Early soybean	0.023	0.065	0.052	0.194	0.281	0.242	0.263	0.369	0.219	0.184	0.267	0.297	0.415	0.283	–	–
Late soybean	0.030	0.073	0.083	0.656	0.402	0.175	0.219	0.263	0.527	0.331	0.537	1.508	2.039	–	–	–

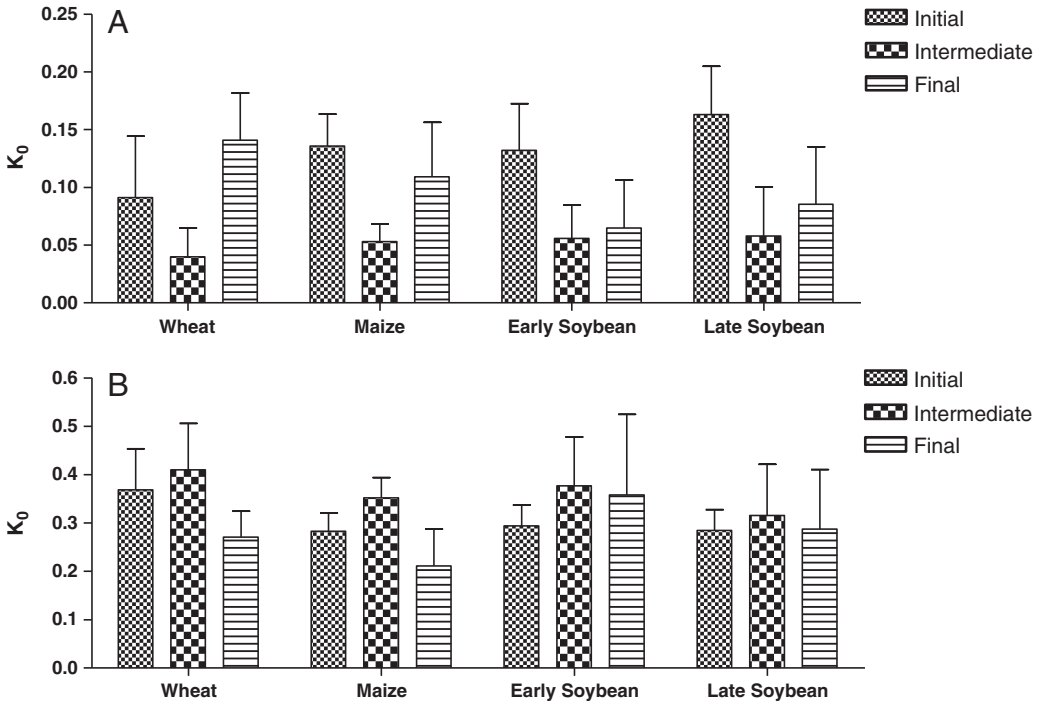

Fig. 5. Crop median k_0 for red (A) and infrared (B) time series for the Classic 3 multiple-period (3MP) correction method. Periods are depicted by different column patterns. Bars represent median absolute deviation (MAD).

4. Discussion

We compared different methods to correct the directional effects that preclude the use of daily MODIS 250 m time-series and showed that reflectance's noise (i.e. high frequency variability) was decreased by 47 to 70% across all methods while corrected NDVI explained a higher proportion of the variability in soybean biomass and fIPAR. Higher reductions were obtained when shorter periods were considered, and results

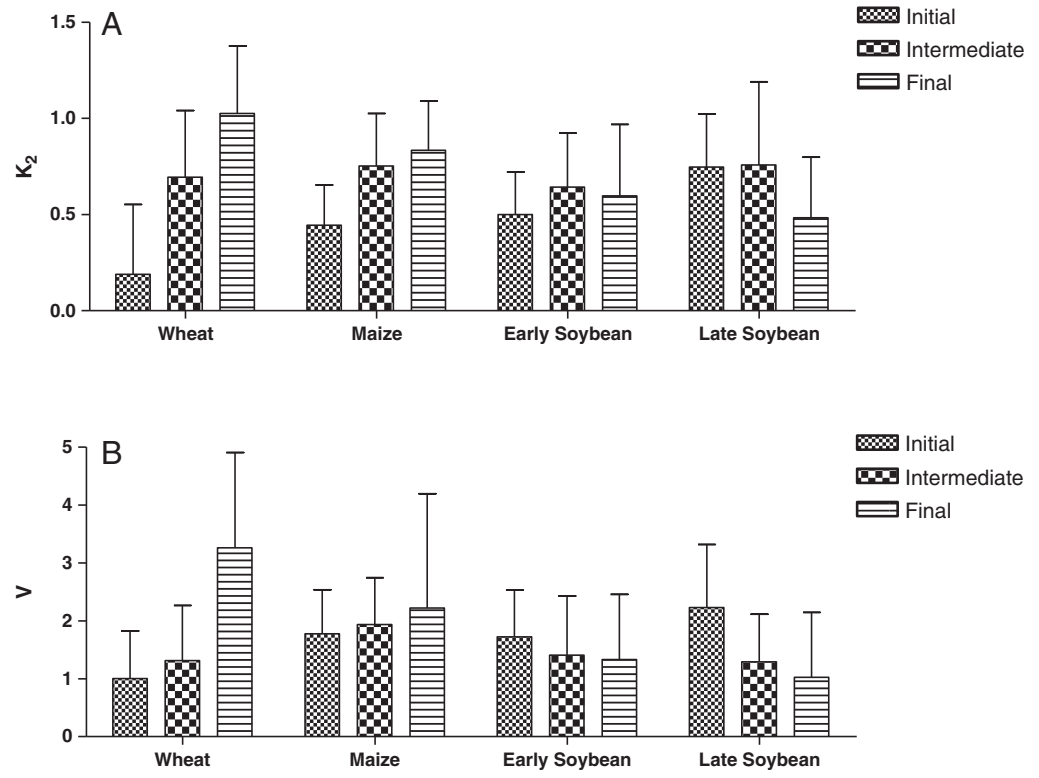

Fig. 6. Crop median of the volumetric parameter k_2 from the Classic 3 multiple-periods (3MP) (A) and of the volumetric V parameter from the Alternative 3 multiple-periods (3MP) (B) correction methods for infrared time-series. Periods are depicted by different column patterns. Bars represent median absolute deviation (MAD).

Table 8
Coefficients of determination for the relation between i) fraction of intercepted photosynthetic active radiation (fIPAR) and the NDVI of the corresponding day ($NDVI_d$, and ii) peak dry biomass and the maximum NDVI ($NDVI_{max}$) for each correction method. In brackets the coefficients of determination are shown when failed pixels (corrected noise higher than uncorrected) were excluded. Superscripts indicate the number of excluded observations.

Dependent variable	Independent variable	Sensor	n	F	CSP	ASP	C3MP	A3MP	C12MP	A12MP
fIPAR	$NDVI_d$	Terra	20	0.31	0.33	0.81	0.49	0.86	0.70	0.77
		Aqua	21	0.76	0.61	0.88	0.68	0.86	0.85	0.87
Peak dry biomass	$NDVI_{max}$	Terra	36	0.48	0.59	0.58	0.54 (0.50)[a]	0.03 (0.51)[b]	0.53	0.06 (0.53)[c]
		Aqua	36	0.52	0.56	0.55	0.47 (0.54)[d]	0.01 (0.48)[e]	0.46 (0.52)[f]	0.01 (0.48)[g]

a: 6, b: 6, c: 11, d: 4, e: 3, f: 3, g: 3.

for Classic and Alternative methods applied over 16-day intervals (12MP methods) were similar. We found that parameters k_x and V and R vary in time and among crops as expected from bidirectional reflectance model theory (Roujean et al., 1992) and thus may have a biological meaning. Our results shed light on the importance of stable target and stable BRDF shape assumptions underlying BRDF correction methods and open the door for the analysis of vegetation dynamics at an unprecedented temporal and spatial resolution.

While undoubtedly more work needs to be done before having an operative methodology to generate corrected daily MODIS reflectance time series, several indicators point to the robustness of our results. Results from two extensively-used quality indices, the high frequency variability and the RMSE, consistently showed that correction methods improved the quality of the time series. In turn, the comparison between different BRDF modeled reflectance to that of LANDSAT provided additional evidence that the BRDF models can acceptably reproduce observed near nadir reflectances. As the ultimate goal of remotely sensed data is to retrieve precise information about the target we also tested whether the corrected time series improved the association to important biophysical variables such as fIPAR and biomass. Indeed, the corrected time series displayed moderate improvements in their associations when compared to the uncorrected time series. Finally, we performed a sensitivity analysis to assess up to what extent our results were influenced by particular thresholds of input data. Its results suggest that most methodologies are stable within an ample range of viewing and illumination angles, Obscov and aerosol quality.

We did not find that the decrease in the noise of red and near infrared reflectances translated into a similar decrease in the noise of the NDVI. Indeed, for the Classic single-period method even an increase in NDVI noise was found. This has been explained on the basis that, being a ratio, the NDVI implicitly contains a directional correction because the effects are similar in the red and infrared reflectances (Vermote et al., 2009). Whenever directional effects cause an increase (decrease) in red and infrared reflectances, NDVI would dampen its effects by canceling a higher (lower) numerator by a higher (lower) denominator. However, it seems implausible that changes in red and infrared reflectances from successive observations would always be positively correlated during a crop cycle. As LAI increases one would expect a decrease in red reflectance – because of chlorophyll absorption – and an increase in infrared reflectance — given the increased cellulose and water scattering (Colwell, 1974; Tucker, 1979). Of course this general pattern of negative correlation may be obscure or reversed by, among other factors, background reflectance, amount of shadow, moisture content and measurement geometry (Colwell, 1974), which may change on a daily time-step. We found a positive correlation (average Pearson moment correlation $r = 0.59$, significant positive $= 562$, significant negative $= 0$, p-value < 0.05) between changes in successive observations of MODIS red and infrared filtered (i.e. no correction) reflectance, while

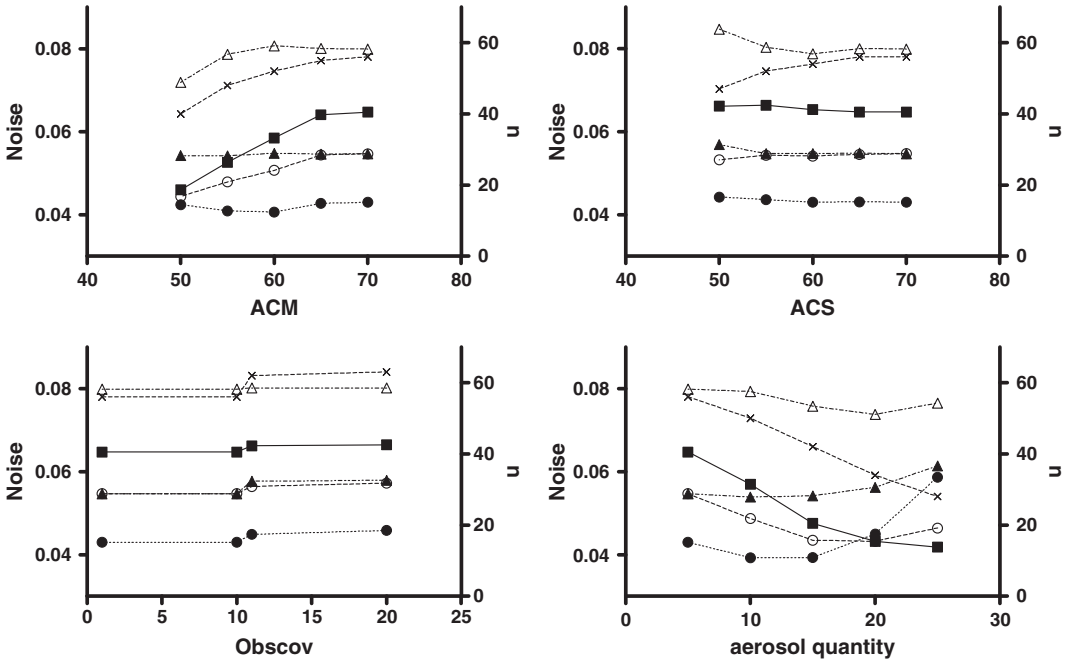

Fig. 7. NDVI noise median (left y-axis) and total number of observations (right y-axis) as a function of the threshold value used to filter each parameter (viewing or illumination angle, aerosol quantity or observation coverage) keeping constant the rest of the parameters. Squares: input filtered data (no corrected); crosses: number of data of the filtered time-series. Triangles: Classic correction methods and circles: Alternative correction methods. Open symbols: simple-period (SP) and filled symbols: 3 multiple-periods (3MP).

Appendix 1

Table A1
Parameters describing absolute high frequency variability (noise) of red, infrared and NDVI time series. F: filtered (uncorrected data), CSP (Classic single period), ASP: Alternative single period, C3MP: Classic 3 multiple-periods, A3MP: Alternative 3 multiple-periods, C12MP: Classic 9–12 multiple-periods, A12MP: Alternative 9–12 multiple-periods.

Band	Red							Infrared			
Method	F	CSP	ASP	C3MP	A3MP	C12MP	A12MP	F	CSP	ASP	C3MP
Mean	0.028	0.016	0.015	0.012	0.015	0.010	0.017	0.077	0.043	0.032	0.031
Standard deviation	0.006	0.006	0.024	0.003	0.036	0.003	0.045	0.012	0.019	0.011	0.010
Median	0.028	0.015	0.012	0.011	0.010	0.010	0.010	0.077	0.039	0.030	0.030
Median absolute deviation	0.006	0.005	0.004	0.003	0.004	0.003	0.004	0.012	0.016	0.010	0.010
Percentile 05	0.018	0.009	0.007	0.007	0.006	0.006	0.005	0.056	0.020	0.017	0.017
Percentile 95	0.038	0.026	0.026	0.018	0.027	0.016	0.044	0.097	0.080	0.053	0.050
Number of observations	2628	2628	2628	2448	2448	2448	2448	2628	2628	2628	2448

for the Alternative methods there was no consistent correlation (average $r = 0.038$ and 0.045, significant positive = 349 and 361, significant negative = 231 and 235 for SP and 3MP respectively, p-value < 0.05) or negative in case of Classic methods (average $r = -0.19$ and -0.13, significant positive = 139 and 145, significant negative = 746 and 696 for SP and 3MP respectively, p-value < 0.05). In addition, we tested whether the reduction in the short term variability was due to the formulation of the NDVI or to the type of correlation (i.e. positive or negative) between red and infrared reflectances by generating randomly correlated time series. NDVI noise resulted systematically lower when red and infrared time-series were positively correlated than when they were negatively or no correlated. On the other hand, the noise from the simple ratio index (IR/R) showed no association with the type of correlation between reflectances. Therefore, the remaining noise of the NDVI constructed from corrected red and infrared reflectances may contain valuable information on short term changes in vegetation status.

Our results also highlight the importance of the number of periods used to characterize the BRDF function. As expected, the noise reduction in Classic method improved significantly when 3 or 9–12 periods instead of 1 were considered in line with the idea that during the crop cycle vegetation does not remain stable. The Alternative method, which assumes that the BRDF shape and not the target remains stable, also improved (although less), when 3 or 9–12 periods were considered. Vermote et al. (2009) found similarly reductions in noise when using multiple periods based on NDVI ranges to correct 3 years of reflectance data from a 25 km^2 of savanna vegetation. These converging

Table A2
Parameters describing relative high frequency variability (noise) of red, infrared and NDVI time series for correction methods that could be applied in the majority of pixels for each crop. F: filtered (uncorrected data), CSP (Classic single period), ASP: Alternative single period, C3MP: Classic 3 multiple-periods, A3MP: Alternative 3 multiple-periods, C12MP: Classic 9–12 multiple-periods, A12MP: Alternative 9–12 multiple-periods.

Band	Red							Infrared			
Method	F	CSP	ASP	C3MP	A3MP	C12MP	A12MP	F	CSP	ASP	C3MP
Crop: wheat											
Mean	0.411	0.256	0.294	0.189	0.377	0.180	0.532	0.228	0.170	0.108	0.107
Standard deviation	0.125	0.108	0.265	0.058	0.643	0.055	2.158	0.050	0.061	0.044	0.028
Median	0.394	0.239	0.231	0.184	0.209	0.173	0.219	0.221	0.168	0.103	0.105
Median absolute deviation	0.109	0.090	0.129	0.048	0.111	0.046	0.133	0.037	0.062	0.033	0.026
Percentile 05	0.235	0.107	0.077	0.091	0.080	0.087	0.078	0.169	0.066	0.058	0.067
Percentile 95	0.639	0.438	0.610	0.291	1.020	0.277	1.611	0.310	0.269	0.171	0.155
Number of observations	666	666	666	486	486	486	486	666	666	666	486
Crop: maize											
Mean	0.393	0.255	0.243	0.176	0.194	0.154	0.216	0.271	0.158	0.125	0.105
Standard deviation	0.128	0.187	0.202	0.117	0.266	0.114	0.419	0.042	0.042	0.040	0.030
Median	0.382	0.244	0.216	0.163	0.165	0.143	0.141	0.265	0.154	0.116	0.101
Median absolute deviation	0.044	0.059	0.075	0.052	0.063	0.046	0.061	0.043	0.040	0.034	0.031
Percentile 05	0.316	0.156	0.124	0.101	0.087	0.085	0.073	0.216	0.098	0.077	0.065
Percentile 95	0.482	0.359	0.395	0.272	0.318	0.234	0.489	0.341	0.238	0.206	0.165
Number of observations	446	446	446	446	446	446	446	446	446	446	446
Crop: early soybean											
Mean	0.399	0.237	0.232	0.191	0.237	0.172	0.241	0.247	0.123	0.103	0.098
Standard deviation	0.065	0.088	0.107	0.056	0.361	0.058	0.399	0.039	0.043	0.034	0.032
Median	0.392	0.219	0.208	0.182	0.168	0.162	0.155	0.241	0.113	0.099	0.093
Median absolute deviation	0.058	0.067	0.089	0.045	0.070	0.048	0.070	0.032	0.040	0.031	0.031
Percentile 05	0.305	0.132	0.107	0.116	0.089	0.099	0.080	0.196	0.072	0.056	0.053
Percentile 95	0.512	0.426	0.428	0.295	0.465	0.279	0.625	0.318	0.201	0.166	0.158
Number of observations	878	878	878	878	878	878	878	878	878	878	878
Crop: late soybean											
Mean	0.399	0.235	0.221	0.206	0.233	0.177	0.298	0.230	0.118	0.102	0.098
Standard deviation	0.074	0.078	0.102	0.063	0.371	0.064	0.610	0.050	0.046	0.039	0.035
Median	0.395	0.225	0.207	0.197	0.159	0.163	0.151	0.225	0.109	0.093	0.090
Median absolute deviation	0.065	0.076	0.096	0.065	0.064	0.059	0.068	0.052	0.038	0.034	0.028
Percentile 05	0.289	0.125	0.101	0.118	0.088	0.096	0.081	0.156	0.065	0.057	0.058
Percentile 95	0.537	0.374	0.436	0.311	0.490	0.300	0.910	0.304	0.220	0.179	0.169
Number of observations	638	638	638	638	638	638	638	638	638	638	638

			NDVI						
A3MP	C12 P	A12MP	F	CSP	ASP	C3MP	A3MP	C12MP	A12MP
0.033	0.028	0.036	0.068	0.083	0.064	0.058	0.061	0.050	0.087
0.092	0.010	0.127	0.021	0.029	0.178	0.016	0.166	0.014	0.400
0.025	0.026	0.023	0.065	0.080	0.055	0.055	0.043	0.048	0.039
0.009	0.009	0.009	0.019	0.028	0.019	0.015	0.016	0.013	0.016
0.014	0.015	0.012	0.040	0.041	0.032	0.036	0.025	0.030	0.023
0.048	0.046	0.053	0.107	0.137	0.101	0.087	0.103	0.077	0.183
2448	2448	2448	2628	2628	2628	2448	2448	2448	2448

results evidence the difficulty of characterizing a dynamic entity as vegetation – and particularly crops – where the possibility of improving the temporal resolution of the BRDF characterization (and improving the correction) is constrained by the availability of good quality observations. The definition of the optimal period's length requires site and vegetation specific knowledge which may introduce a subjective component.

The effect of shorter period upon noise reduction was higher for the Classic than for the Alternative approach (Figs. 1, 2). These results are in line with the assumptions underlying each approach. As the Classic approach assumes a stable target, more problems should be expected for larger periods than for the Alternative methods which assume stable BRDF shape (and not stable target.). From the later, it follows that Alternative methods are more flexible on the definition of the length of the period when the number of available data is low.

Although Alternative methods performed better (lower noise median values), they had a given percentage of pixels with very high noise, and higher standard deviation and mean values than Classic ones (Appendix 1).One reason of this behavior could be that particular combinations of kernels and kernel parameters that are minimized without constrains could give very high values in the correction factor (Eqs. (4) and (5)) and in addition, in the corrected reflectance values. We found situations for the Alternative methods where the correction factor was higher than 3 (implying at least a 200% correction). This issue occurred at least once on 8% of pixels. Classic methods, as they used one more parameter than the Alternative, showed a lower occurrence of this effect

			NDVI						
A3MP	C12MP	A12MP	F	CSP	ASP	C3MP	A3MP	C12MP	A12MP
0.107	0.099	0.134	0.114	0.273	0.545	0.108	0.232	0.101	0.317
0.095	0.027	0.284	0.038	1.004	3.551	0.041	0.912	0.036	1.722
0.092	0.096	0.090	0.107	0.150	0.119	0.097	0.093	0.092	0.095
0.031	0.024	0.033	0.032	0.062	0.051	0.027	0.046	0.022	0.052
0.054	0.060	0.051	0.064	0.073	0.064	0.065	0.046	0.064	0.047
0.178	0.148	0.305	0.182	0.443	0.956	0.179	0.696	0.167	0.795
486	486	486	666	666	666	486	486	486	486
0.140	0.091	0.148	0.156	0.224	0.146	0.134	0.133	0.118	0.171
0.600	0.028	0.635	0.049	0.135	0.051	0.045	0.208	0.041	0.475
0.093	0.087	0.083	0.147	0.212	0.137	0.124	0.104	0.109	0.093
0.031	0.030	0.032	0.051	0.055	0.043	0.038	0.042	0.037	0.041
0.056	0.053	0.049	0.091	0.121	0.082	0.078	0.056	0.067	0.050
0.195	0.145	0.233	0.250	0.341	0.236	0.214	0.211	0.183	0.299
446	446	446	446	446	446	446	446	446	446
0.083	0.084	0.081	0.133	0.364	0.118	0.123	0.136	0.104	0.335
0.045	0.027	0.134	0.039	2.285	0.039	0.039	0.488	0.035	6.619
0.079	0.082	0.067	0.127	0.182	0.112	0.115	0.084	0.099	0.074
0.028	0.028	0.024	0.035	0.083	0.032	0.035	0.028	0.030	0.029
0.043	0.045	0.037	0.079	0.087	0.072	0.070	0.052	0.060	0.043
0.135	0.137	0.125	0.206	0.721	0.190	0.196	0.187	0.158	0.247
878	878	878	878	878	878	878	878	878	878
0.093	0.088	0.082	0.160	7.934	0.539	0.124	0.194	0.113	0.285
0.120	0.030	0.053	0.060	183.5	7.521	0.047	0.800	0.065	1.180
0.078	0.083	0.073	0.146	0.170	0.117	0.115	0.086	0.100	0.083
0.025	0.025	0.025	0.050	0.088	0.047	0.036	0.033	0.033	0.034
0.048	0.052	0.042	0.084	0.079	0.066	0.071	0.049	0.062	0.047
0.151	0.144	0.146	0.273	1.932	0.671	0.208	0.313	0.184	0.800
638	638	638	638	638	638	638	638	638	638

(less than 2% of pixels). Frequency of failed pixels increased with the number of periods considered as a higher number of minimizations was performed.

Wheat displayed the highest percentage of pixels where the correction did not imply a reduction in the reflectance or NDVI noise. There are several reasons that may help to explain this outcome. Wheat in the Pampas grows during a period where clouds or illumination angles may reduce the amount of good quality observations. In fact, wheat showed the lowest percentage of cloudless observations – 31% – compared to 37 for maize and early soybean and 38% and late soybean respectively. The combined effect of less cloud free observations and, on average, high illumination angles occurring at the beginning of the wheat crop cycle may partially explain its relatively poor angular sampling — as evidenced by the high WoD from the first sub-period. Wheat longer growing season could not compensate for this effect, as the total number of good quality observations was, on average 50 for wheat vs. 54, 62 or 71 for late, early soybean and maize respectively. However, wheat did show higher intervals of missing data that could be responsible for its lower performance. In turn, the low sensitivity of correction methods to sun zenith angles suggests that this variable should not be playing an important role to explain wheat performance. Additionally, as the noise from the filtered time series did not differ between crops it can also be discarded that wheat is intrinsically noisier than maize or soybeans.

From Fig. 5 it is apparent that k_0 follows the dynamic of the green biomass showing an infrared maximum and a red minimum at the intermediate period where green biomass is expected to peak. This pattern agrees with the Roujean et al. (1992) definition of k_0: the bidirectional reflectance when both sun and sensor are at nadir. However, at the intermediate period the values of k_0 were not associated to green biomass (as in general maize has more biomass than the other crops) suggesting that other variables such as canopy shadowing or leaf transmittance (Colwell, 1974) may be involved in the determination of k_0.

Gao et al. (2003) suggested that k_2 at infrared band is sensitive to vegetation structure, being higher at dense canopies with few gaps and thus higher volumetric scattering. For 3MP methods, crops showed differences in the values of k_2 at the final period compared to the values at the intermediate period (Fig. 5A). Decrease in k_2 values for soybean could be associated to structural changes that occur at maturity related to leaf abscission. On the contrary, wheat and maize, crops that retain leaves, showed increments in k_2 at the final period. The higher values of k_2 for late compared to early soybean at initial stages could be associated to the presence of standing wheat residues which is common due to the extensive use of direct sowing in the Pampas. V parameter at infrared band showed a similar pattern to k_2 when comparing the intermediate to the final period for 3MP methods (Fig. 5B), and could be also related to changes in vegetation structure. V parameter values, although independently generated, were associated to the temporal variation of k_2 and k_0 values generated for the Classic method (Figs. 4 and 5).

The decrease in noise translated to a better association between NDVI and fIPAR and soybean biomass. However, the influence of failed pixels is evident from the difference in the r^2 obtained considering all against only those where correction resulted in a noise reduction. Therefore, care is needed when performing an operational correction of directional effects using methods that do not assure 100% success. Such an approach could employ more than one correction method to be used when the main correction method fails.

Overall, these results seem promising. The BRDF correction methods tested here represent a significant step forward towards the operational production of high spatiotemporal resolution observations of vegetation. Corrected time-series showed, on average, between 5 and 6 times more observations than those obtained in the standard 16 day compositing period. Moreover, these corrected observations were better correlated with biophysical variables such as soybean biomass than their uncorrected counterparts. We propose that this so called "hyper-temporal" analysis could be particularly useful for monitoring rapid changes in crop status.

Acknowledgments

Our work is funded by INTA (AERN-294421), ANPCyT (PICT 0598) and CONAE (AO SAOCOM N°7). The ideas that lead to this manuscript were developed within the JECAM (Joint Experiment for Crop Assessment and Monitoring) initiative. The authors thank NASA for sharing MODIS data through Reverb. Mark Chopping provided valuable help with WoD calculation. We very much appreciate the contributions made by three anonymous reviewers whose comments and suggestions significantly improved this manuscript.

References

Becker-Reshef, I., Vermote, E., Lindeman, M., & Justice, C. (2010). A generalized regression-based model for forecasting winter wheat yields in Kansas and Ukraine using MODIS data. *Remote Sensing of Environment*, *114*, 1312–1323.

Breon, F. M., Maignan, F., Leroy, M., & Grant, I. (2002). Analysis of hot spot directional signatures measured from space. *Journal of Geophysical Research*, *107*, 4282.

Breon, F. M., & Vermote, E. (2012). Correction of MODIS surface reflectance time series for BRDF effects. *Remote Sensing of Environment*, *125*, 1–9.

Chandler, G., & Markham, B. (2003). Revised Landsat 5-TM radiometric calibration procedures and postcalibration dynamics. *IEEE Transactions on Geoscience and Remote Sensing*, *41*, 2674–2677.

Chopping, M. (2000). Testing a LiSK BRDF model with in situ bidirectional reflectance factor measurements over semiarid grasslands. *Remote Sensing of Environment*, *74*, 287–312.

Colwell, J. E. (1974). Vegetation canopy reflectance. *Remote Sensing of Environment*, *3*, 175–183.

Darecki, M., & Stramski, D. (2004). An evaluation of MODIS and SeaWiFS bio-optical algorithms in the Baltic Sea. *Remote Sensing of Environment*, *89*, 326–350.

Friedl, M.A., McIver, D. K., Hodges, J. C. F., Zhang, X. Y., Muchoney, D., Strahler, A. H., et al. (2002). Global land cover mapping from MODIS: Algorithms and early results. *Remote Sensing of Environment*, *83*, 287–302.

Gao, F., Schaaf, C. B., Strahler, A. H., Jin, Y., & Li, X. (2003). Detecting vegetation structure using a kernel-based BRDF model. *Remote Sensing of Environment*, *86*, 198–205.

Huete, A., Didan, K., van Leeuwen, W., Miura, T., & Glenn, E. (2011). MODIS vegetation indices. In B. Ramachandran, C. O. Justice, & M. J. Abrams (Eds.), *Land remote sensing and global environmental change* (pp. 579–602). New York: Springer.

Kaufman, Y. J., Tanré, D., & Boucher, O. (2002). A satellite view of aerosols in the climate system. *Nature*, *419*, 215–223.

King, M.D., Menzel, W. P., Kaufman, Y. J., Tanré, D., Gao, B. -C., Platnick, S., et al. (2003). Cloud and aerosol properties, precipitable water, and profiles of temperature and water vapor from MODIS. *IEEE Transactions on Geoscience and Remote Sensing*, *41*, 442–458.

Li, X., & Strahler, A. H. (1992). Geometric — Optical bidirectional reflectance modeling of the discrete crown vegetation canopy: Effect of crown shape and mutual shadowing. *IEEE Transactions on Geoscience and Remote Sensing*, *30*, 276–292.

Lucht, W., & Lewis, P. (2000). Theoretical noise sensitivity of BRDF and Albedo retrieval from the EOS-MODIS and MISR sensors with respect to angular sampling. *International Journal of Remote Sensing*, *21*, 81–98.

Pittman, K., Hansen, M. C., Becker-Reshef, I., Potapov, P. V., & Justice, C. O. (2010). Estimating global cropland extent with multi-year MODIS data. *Remote Sensing*, *2*, 1844–1863.

Rasmussen, M.O., Göttsche, F. -M., Olesen, F. -S., & Sandholt, I. (2011). Directional effects on land surface temperature estimation from Meteosat Second Generation for savanna landscapes. *IEEE Transactions on Geoscience and Remote Sensing*, *49*, 4458–4468.

Ross, J. K. (1981). *The radiation regime and architecture of plant stands*. The Hague–Boston–London: W. Junk Publishers, 391.

Roujean, J., Leroy, M., & Deschamps, P. (1992). A bidirectional reflectance model of the earth's surface for the correction of remote sensing data. *Journal of Geophysical Research*, *97* (20.455-420.468).

Roy, D., Lewis, P., & Justice, C. (2002). Burned area mapping using multi-temporal moderate spatial resolution data—a bi-directional reflectance model-based expectation approach. *Remote Sensing of Environment*, *83*, 263–286.

Salomonson, V., Abrams, M. J., Kahle, A., Barnes, W., Xiong, X., Yamaguchi, Y., et al. (2011). Evolution of NASA's earth observing system and development of the moderate-resolution imaging spectroradiometer and the advanced spaceborne thermal emission and reflection radiometer instruments. In F. D. Meer, & A. Marçal (Eds.), *Land remote sensing and global environmental change* (pp. 3–34). New York: Springer.

Schaaf, C. B., Gao, F., Strahler, A. H., Lucht, W., Li, X., Tsang, T., et al. (2002). First operational BRDF, albedo nadir reflectance products from MODIS. *Remote Sensing of Environment*, *83*, 135–148.

Schaepman-Strub, G., Schaepman, M. E., Painter, T. H., Dangel, S., & Martonchik, J. V. (2006). Reflectance quantities in optical remote sensing: Definitions and case studies. *Remote Sensing of Environment*, *103*, 27–42.

Shuai, Y., Schaaf, C., Strahler, A. H., Liu, J., & Jiao, Z. (2008). Quality assessment of BRDF/albedo retrievals in MODIS operational system. *Geophysical Research Letters*, *35*, L05407.

Stumpf, R. P. (1992). Remote sensing of water clarity and suspended sediments in coastal waters. *Proceedings of the First Thematic Conference on Remote Sensing for Marine and Coastal Environments*. Ann Arbor, Michigan: Environmental Research Institute of Michigan.

Tucker, C. J. (1979). Red and photographic infrared linear combinations for monitoring vegetation. *Remote Sensing of Environment*, *8*, 127–150.

Van Der Werf, G. R., Randerson, J. T., Giglio, L., Collatz, G. J., Kasibhatla, P.S., & Arellano, A. F., Jr. (2006). Interannual variability in global biomass burning emissions from 1997 to 2004. *Atmospheric Chemistry and Physics*, *6*, 3423–3441.

Vermote, E., Justice, C. O., & Breon, F. M. (2009). Towards a generalized approach for correction of the BRDF effect in MODIS directional reflectances. *IEEE Transactions on Geoscience and Remote Sensing*, *47*, 898–908.

Zhang, X., Friedl, M.A., Schaaf, C. B., Strahler, A. H., Hodges, J. C. F., Gao, F., et al. (2003). Monitoring vegetation phenology using MODIS. *Remote Sensing of Environment*, *84*, 471–475.